

Doping and energy evolution of spin dynamics in the electron-doped cuprate superconductor $\text{Pr}_{0.88}\text{LaCe}_{0.12}\text{CuO}_{4-\delta}$

Li Cheng and Shiping Feng*

Department of Physics, Beijing Normal University, Beijing 100875, People's Republic of China

(Received 15 November 2007; revised manuscript received 7 January 2008; published 27 February 2008)

The doping and energy evolution of the magnetic excitations of the electron-doped cuprate superconductor $\text{Pr}_{0.88}\text{LaCe}_{0.12}\text{CuO}_{4-\delta}$ in the superconducting state is studied based on the kinetic energy driven superconducting mechanism. It is shown that there is a broad commensurate scattering peak at low energy, then the resonance energy is located among this low energy commensurate scattering range. This low energy commensurate scattering disperses outward into a continuous ringlike incommensurate scattering at high energy. The theory also predicts a dome shaped doping dependent resonance energy.

DOI: [10.1103/PhysRevB.77.054518](https://doi.org/10.1103/PhysRevB.77.054518)

PACS number(s): 74.62.Dh, 74.20.Mn, 74.25.Ha

I. INTRODUCTION

The parent compounds of cuprate superconductors are believed to belong to a class of materials known as Mott insulators with an antiferromagnetic (AF) long-range order; then, superconductivity emerges when charge carriers, holes, or electrons are doped into these Mott insulators.^{1,2} It has been found that only an approximate symmetry in the phase diagram exists about the zero doping line between the hole-doped and electron-doped cuprate superconductors, and the significantly different behavior of the hole-doped and electron-doped cases is observed,³ reflecting the electron-hole asymmetry.

Experimentally, by virtue of systematic studies using the nuclear magnetic resonance and muon spin rotation techniques, particularly the inelastic neutron scattering (INS), the dynamical spin response in the hole-doped and electron-doped cuprate superconductors in the superconducting (SC) state has been well established now,⁴⁻¹⁰ where an important issue is whether the behavior of the magnetic excitations determined by the dynamical spin structure factor (DSSF) is universal or not. The early INS measurements on the hole-doped cuprate superconductors⁴⁻⁷ showed that the low energy spin fluctuations form a quarter of the incommensurate (IC) magnetic scattering peaks at wave vectors away from the AF wave vector $[\pi, \pi]$ (in units of inverse lattice constant). With increasing energy, these IC magnetic scattering peaks are converged on the commensurate $[\pi, \pi]$ resonance peak at intermediate energy. Well above this resonance energy, the continuum of the spin-wave-like IC magnetic excitations is observed. Very recently, the INS measurements on the electron-doped cuprate superconductor $\text{Pr}_{0.88}\text{LaCe}_{0.12}\text{CuO}_{4-\delta}$ (Refs. 8-10) showed that the IC magnetic scattering and inward dispersion toward a resonance peak with increasing energy appeared in the hole-doped cuprate superconductors are not observed in the electron-doped side. Instead, the magnetic scattering in the electron-doped cuprate superconductor $\text{Pr}_{0.88}\text{LaCe}_{0.12}\text{CuO}_{4-\delta}$ has a broad commensurate peak centered at $[\pi, \pi]$ at low energy (≤ 50 meV). In particular, the magnetic resonance is located among this low energy broad commensurate scattering range. In analogy to the hole-doped cuprate superconductors, the commensurate resonance with the resonance energy

(~ 10 meV) in the electron-doped side scales with the SC transition temperature, forming a universal plot for all cuprate superconductors irrespective of the hole-doped and electron-doped cases. Furthermore, the low energy broad commensurate magnetic scattering disperses outward into a continuous ringlike IC magnetic scattering at high energy ($50 \text{ meV} < \omega < 300 \text{ meV}$); this is the same as the hole-doped case. Therefore, the hour-glass-shaped dispersion in the magnetic scattering of the hole-doped superconductors may not be a universal and intrinsic feature of all cuprate superconductors.⁸⁻¹⁰ Instead, the commensurate resonance itself appears to be a universal property of cuprate superconductors.⁸⁻¹⁰ At present, it is not clear how theoretical models based on a microscopic SC theory can reconcile the difference of the dynamical spin response in the hole-doped and electron-doped cuprate superconductors. No explicit predictions on the doping dependence of the resonance energy in the electron-doped cuprate superconductors have been made so far.

Within the framework of the kinetic energy driven SC mechanism,¹¹ the dynamical spin response of the hole-doped cuprate superconductors has been discussed,¹² and the results are in qualitative agreement with the INS experimental data.⁴⁻⁷ In this paper, we study the doping and energy dependence of the spin dynamics in the electron-doped cuprate superconductor $\text{Pr}_{0.88}\text{LaCe}_{0.12}\text{CuO}_{4-\delta}$ along with this line. We calculate explicitly the DSSF of the electron-doped cuprate superconductor $\text{Pr}_{0.88}\text{LaCe}_{0.12}\text{CuO}_{4-\delta}$ and reproduce qualitatively all main features of the INS experiments on the electron-doped cuprate superconductor $\text{Pr}_{0.88}\text{LaCe}_{0.12}\text{CuO}_{4-\delta}$ in the SC state,⁸⁻¹⁰ including the energy dependence of the commensurate magnetic scattering and resonance at low energy and IC magnetic scattering at high energy. Our results also show that the difference of the low energy dynamical spin response between the hole-doped and electron-doped cuprate superconductors is mainly caused by the SC gap function in the electron-doped case deviated from the monotonic d -wave function.

The rest of this paper is organized as follows. The basic formalism is presented in Sec. II, where we generalize the calculation of the DSSF from the previous hole-doped case¹² to the present electron-doped case. Within this theoretical framework, we discuss the dynamical spin response of the

electron-doped cuprate superconductor $\text{Pr}_{0.88}\text{LaCe}_{0.12}\text{CuO}_{4-\delta}$ in the SC state in Sec. III, where we predict a dome shaped doping dependent resonance energy. Finally, we give summary and discussions in Sec. IV.

II. THEORETICAL FRAMEWORK

In both hole-doped and electron-doped cuprate superconductors, the characteristic feature is the presence of the two-dimensional CuO_2 plane,¹⁻³ and it seems evident that the unusual behaviors of cuprate superconductors are dominated by this plane. From the angle-resolved photoemission spectroscopy (ARPES) experiments,^{3,13} it has been shown that the essential physics of the CuO_2 plane in the electron-doped cuprate superconductors is contained in the t - t' - J model on a square lattice,

$$H = t \sum_{i\hat{\eta}\sigma} P C_{i\sigma}^\dagger C_{i+\hat{\eta}\sigma} P^\dagger - t' \sum_{i\hat{\tau}\sigma} P C_{i\sigma}^\dagger C_{i+\hat{\tau}\sigma} P^\dagger - \mu \sum_{i\sigma} P C_{i\sigma}^\dagger C_{i\sigma} P^\dagger + J \sum_{i\hat{\eta}} \mathbf{S}_i \cdot \mathbf{S}_{i+\hat{\eta}}, \quad (1)$$

where $t < 0$, $t' < 0$, $\hat{\eta} = \pm \hat{x}, \pm \hat{y}$, $\hat{\tau} = \pm \hat{x} \pm \hat{y}$, $C_{i\sigma}^\dagger$ ($C_{i\sigma}$) is the electron creation (annihilation) operator, $\mathbf{S}_i = C_i^\dagger \vec{\sigma} C_i / 2$ is the spin operator with $\vec{\sigma} = (\sigma_x, \sigma_y, \sigma_z)$ as Pauli matrices, μ is the chemical potential, and the projection operator P removes zero occupancy, i.e., $\sum_\sigma C_{i\sigma}^\dagger C_{i\sigma} \geq 1$. In this case, an important question is the relation between the hole-doped and electron-doped cases. The t - J model with nearest-neighbor hopping t has a particle-hole symmetry because the sign of t can be absorbed by changing the sign of the orbital on one sublattice. However, the particle-hole asymmetry can be described by including the next neighbor hopping t' , which has been tested extensively in Ref. 14, where they use *ab initio* local density functional theory to generate input parameters for the three-band Hubbard model and then solve the spectra exactly on finite clusters, and the results are compared with the low energy spectra of the one-band Hubbard model and the t - t' - J model. They^{14,15} found an excellent overlap of the low lying wave functions for both the one-band Hubbard model and the t - t' - J model, and were able to extract the effective parameters as $J \approx 0.1 \sim 0.13$ eV, $t/J = 2.5 \sim 3$ for the hole doping and $t/J = -2.5$ to -3 for the electron doping, and t'/t is of order 0.2–0.3 and is believed to vary somewhat from compound to compound. Although there is a similar strength of the magnetic interaction J for both hole-doped and electron-doped cuprate superconductors, the interplay of t' with t and J causes a further weakening of the AF spin correlation for the hole doping and enhancing the AF spin correlation for the electron doping,¹⁴⁻¹⁶ therefore, the AF spin correlations in the electron-doped case are stronger than those in the hole-doped side. In particular, it has been shown from the ARPES experiments that the lowest energy states in the hole-doped cuprate superconductors in the normal state are located at $\mathbf{k} = [\pi/2, \pi/2]$ point, while they appear at $\mathbf{k} = [\pi, 0]$ point in the electron-doped case.^{3,13} This asymmetry seen by the ARPES observation on the hole-doped and electron-doped cuprates is actually consistent with calculations performed within the t - t' - J model based on the exact diagonalization

studies,¹³ where all of the hopping terms have opposite signs for the electron and hole doping, and the sign of t' is of crucial importance for the coupling of the charge motion to the spin background. Furthermore, the low energy electronic structures of the hole-doped and electron-doped cuprates have been well reproduced by the mean-field (MF) solutions within the t - t' - J model.¹⁷

For the hole-doped case, the charge-spin separation (CSS) fermion-spin theory has been developed to incorporate the single occupancy constraint.¹⁸ In particular, it has been shown that under the decoupling scheme, this CSS fermion-spin representation is a natural representation of the constrained electron defined in a restricted Hilbert space without double electron occupancy.¹⁹ To apply this theory in the electron-doped case, the t - t' - J model [Eq. (1)] can be rewritten in terms of a particle-hole transformation $C_{i\sigma} \rightarrow f_{i-\sigma}^\dagger$ as

$$H = -t \sum_{i\hat{\eta}\sigma} f_{i\sigma}^\dagger f_{i+\hat{\eta}\sigma} + t' \sum_{i\hat{\tau}\sigma} f_{i\sigma}^\dagger f_{i+\hat{\tau}\sigma} - \mu \sum_{i\sigma} f_{i\sigma}^\dagger f_{i\sigma} + J \sum_{i\hat{\eta}} \mathbf{S}_i \cdot \mathbf{S}_{i+\hat{\eta}}, \quad (2)$$

supplemented by a local constraint $\sum_\sigma f_{i\sigma}^\dagger f_{i\sigma} \leq 1$ to remove double occupancy, where $f_{i\sigma}^\dagger$ ($f_{i\sigma}$) is the hole creation (annihilation) operator, while $\mathbf{S}_i = f_i^\dagger \vec{\sigma} f_i / 2$ is the spin operator in the hole representation. Now, we follow the CSS fermion-spin theory¹⁸ and decouple the hole operators as $f_{i\uparrow} = a_{i\uparrow}^\dagger S_i^-$ and $f_{i\downarrow} = a_{i\downarrow}^\dagger S_i^+$, where the spinful fermion operator $a_{i\sigma} = e^{-i\Phi_{i\sigma}} a_i$ describes the charge degree of freedom together with some effects of spin configuration rearrangements due to the presence of the doped electron itself (dressed charge carrier), while the spin operator S_i describes the spin degree of freedom; then, the single occupancy local constraint is satisfied. In this CSS fermion-spin representation, the t - t' - J model [Eq. (2)] can be expressed as

$$H = -t \sum_{i\hat{\eta}} (a_{i\uparrow} S_i^+ a_{i+\hat{\eta}\uparrow}^\dagger S_{i+\hat{\eta}}^- + a_{i\downarrow} S_i^- a_{i+\hat{\eta}\downarrow}^\dagger S_{i+\hat{\eta}}^+) + t' \sum_{i\hat{\tau}} (a_{i\uparrow} S_i^+ a_{i+\hat{\tau}\uparrow}^\dagger S_{i+\hat{\tau}}^- + a_{i\downarrow} S_i^- a_{i+\hat{\tau}\downarrow}^\dagger S_{i+\hat{\tau}}^+) - \mu \sum_{i\sigma} a_{i\sigma}^\dagger a_{i\sigma} + J_{\text{eff}} \sum_{i\hat{\eta}} \mathbf{S}_i \cdot \mathbf{S}_{i+\hat{\eta}}, \quad (3)$$

with $J_{\text{eff}} = (1-x)^2 J$ and $x = \langle a_{i\sigma}^\dagger a_{i\sigma} \rangle = \langle a_i^\dagger a_i \rangle$ is the electron doping concentration. As in the hole-doped case, the SC order parameter for the electron Cooper pair in the electron-doped case also can be defined as

$$\Delta = \langle C_{i\uparrow}^\dagger C_{j\downarrow}^\dagger - C_{i\downarrow}^\dagger C_{j\uparrow}^\dagger \rangle = \langle a_{i\uparrow} a_{j\downarrow} S_i^+ S_j^- - a_{i\downarrow} a_{j\uparrow} S_i^- S_j^+ \rangle = -\langle S_i^+ S_j^- \rangle \Delta_a, \quad (4)$$

with the charge carrier pairing order parameter $\Delta_a = \langle a_{j\downarrow} a_{i\uparrow} - a_{j\uparrow} a_{i\downarrow} \rangle$. It has been shown from the ARPES experiments that the hot spots are located close to $[\pm\pi, 0]$ and $[0, \pm\pi]$ in the hole-doped cuprate superconductors, resulting in a monotonic d -wave gap function.²⁰ In contrast, the hot spots are located much closer to the zone diagonal in the electron-doped case, leading to a nonmonotonic d -wave gap function,²¹

$$\Delta(\mathbf{k}) = \Delta[\gamma_{\mathbf{k}}^{(d)} - B\gamma_{\mathbf{k}}^{(2d)}], \quad (5)$$

with $\gamma_{\mathbf{k}}^{(d)} = [\cos k_x - \cos k_y]/2$ and $\gamma_{\mathbf{k}}^{(2d)} = [\cos(2k_x) - \cos(2k_y)]/2$; then, the maximum SC gap is observed not at the Brillouin-zone boundary, as expected from the monotonic d -wave SC gap function, but at the hot spot between $[\pi, 0]$ and $[\pi/2, \pi/2]$, where the AF spin fluctuation most strongly couples to electrons, suggesting a spin-mediated pairing mechanism.²¹

Within the CSS fermion-spin theory,¹⁸ the kinetic energy driven superconductivity has been developed.¹¹ It has been shown that the interaction from the kinetic energy term in the t - t' - J model [Eq. (3)] is quite strong and can induce the dressed charge carrier pairing state by exchanging spin excitations in the higher power of the doping concentration; then, the electron Cooper pairs originating from the dressed charge carrier pairing state are due to the charge-spin recombination, and their condensation reveals the SC ground state. In particular, this SC state is controlled by both the SC gap function and the quasiparticle coherence, which leads to the fact that the SC transition temperature increases with increasing doping in the underdoped regime, reaches a maximum in the optimal doping, and then decreases in the overdoped regime.¹² Furthermore, superconductivity in the electron-doped cuprate superconductors has also been discussed²² under this kinetic energy driven SC mechanism, and the results show that superconductivity appears over a narrow range of doping, around the optimal electron doping $x=0.15$. Within the kinetic energy driven SC mechanism,¹¹ the DSSF of the hole-doped t - t' - J model in the SC state with a monotonic d -wave gap function has been calculated in terms of the collective mode in the dressed charge carrier particle-particle channel,¹² and the results are in qualitative agreement with the INS experimental data on the hole-doped cuprate superconductors in the SC state.⁴⁻⁷ Following their discussions,¹² we can obtain the DSSF of the electron-doped t - t' - J model [Eq. (3)] in the SC state with the nonmonotonic d -wave gap function [Eq. (5)] as

$$S(\mathbf{k}, \omega) = -2[1 + n_B(\omega)]\text{Im} D(\mathbf{k}, \omega), \quad (6)$$

with the full spin Green's function in the SC state,

$$D(\mathbf{k}, \omega) = \frac{B_{\mathbf{k}}}{\omega^2 - \omega_{\mathbf{k}}^2 - B_{\mathbf{k}}\Sigma^{(s)}(\mathbf{k}, \omega)}, \quad (7)$$

where $B_{\mathbf{k}} = 2\lambda_1(A_1\gamma_{\mathbf{k}} - A_2) - \lambda_2(2\chi_2^z\gamma_{\mathbf{k}}' - \chi_2)$, $\lambda_1 = 2ZJ_{\text{eff}}$, $\lambda_2 = 4Z\phi_2t'$, $A_1 = \epsilon\chi_1^z + \chi_1/2$, $A_2 = \chi_1^z + \epsilon\chi_1/2$, $\epsilon = 1 + 2t\phi_1/J_{\text{eff}}$, $\gamma_{\mathbf{k}} = (1/Z)\sum_{\hat{\eta}} e^{i\mathbf{k}\cdot\hat{\eta}}$, $\gamma_{\mathbf{k}}' = (1/Z)\sum_{\hat{\eta}} e^{i\mathbf{k}\cdot\hat{\eta}}$, Z is the number of the nearest-neighbor or next-nearest-neighbor sites, the dressed charge carrier particle-hole parameters $\phi_1 = \langle a_{i\sigma}^\dagger a_{i+\hat{\eta}\sigma} \rangle$ and $\phi_2 = \langle a_{i\sigma}^\dagger a_{i+\hat{\eta}\sigma} \rangle$, the spin correlation functions $\chi_1 = \langle S_i^+ S_{i+\hat{\eta}}^- \rangle$, $\chi_2 = \langle S_i^+ S_{i+\hat{\eta}}^- \rangle$, $\chi_1^z = \langle S_i^z S_{i+\hat{\eta}}^z \rangle$, and $\chi_2^z = \langle S_i^z S_{i+\hat{\eta}}^z \rangle$, and the MF spin excitation spectrum

$$\begin{aligned} \omega_{\mathbf{k}}^2 = & \lambda_1^2 \left[\left(A_4 - \alpha\epsilon\chi_1^z\gamma_{\mathbf{k}} - \frac{1}{2Z}\alpha\epsilon\chi_1 \right) (1 - \epsilon\gamma_{\mathbf{k}}) \right. \\ & \left. + \frac{1}{2}\epsilon \left(A_3 - \frac{1}{2}\alpha\chi_1^z - \alpha\chi_1\gamma_{\mathbf{k}} \right) (\epsilon - \gamma_{\mathbf{k}}) \right] \\ & + \lambda_2^2 \left[\alpha \left(\chi_2^z\gamma_{\mathbf{k}}' - \frac{3}{2Z}\chi_2 \right) \gamma_{\mathbf{k}}' + \frac{1}{2} \left(A_5 - \frac{1}{2}\alpha\chi_2^z \right) \right] \\ & + \lambda_1\lambda_2 \left[\alpha\chi_1^z(1 - \epsilon\gamma_{\mathbf{k}})\gamma_{\mathbf{k}}' + \frac{1}{2}\alpha(\chi_1\gamma_{\mathbf{k}}' - C_3)(\epsilon - \gamma_{\mathbf{k}}) \right. \\ & \left. + \alpha\gamma_{\mathbf{k}}'(C_3 - \epsilon\chi_2^z\gamma_{\mathbf{k}}) - \frac{1}{2}\alpha\epsilon(C_3 - \chi_2\gamma_{\mathbf{k}}) \right], \quad (8) \end{aligned}$$

with $A_3 = \alpha C_1 + (1 - \alpha)/(2Z)$, $A_4 = \alpha C_1^z + (1 - \alpha)/(4Z)$, $A_5 = \alpha C_2 + (1 - \alpha)/(2Z)$, and the spin correlation functions $C_1 = (1/Z^2)\sum_{\hat{\eta}, \hat{\eta}'} \langle S_{i+\hat{\eta}}^+ S_{i+\hat{\eta}'}^- \rangle$, $C_1^z = (1/Z^2)\sum_{\hat{\eta}, \hat{\eta}'} \langle S_{i+\hat{\eta}}^z S_{i+\hat{\eta}'}^z \rangle$, $C_2 = (1/Z^2)\sum_{\hat{\tau}, \hat{\tau}'} \langle S_{i+\hat{\tau}}^+ S_{i+\hat{\tau}'}^- \rangle$, $C_3 = (1/Z)\sum_{\hat{\tau}} \langle S_{i+\hat{\tau}}^+ S_{i+\hat{\tau}}^- \rangle$, and $C_3^z = (1/Z)\sum_{\hat{\tau}} \langle S_{i+\hat{\tau}}^z S_{i+\hat{\tau}}^z \rangle$. In order to satisfy the sum rule of the correlation function $\langle S_i^+ S_i^- \rangle = 1/2$ in the case without AF long-range order, the decoupling parameter α has been introduced,¹² which can be regarded as the vertex correction, while the spin self-energy function $\Sigma^{(s)}(\mathbf{k}, \omega)$ in Eq. (7) is obtained from the dressed charge carrier bubble in the dressed charge carrier particle-particle channel as

$$\begin{aligned} \Sigma^{(s)}(\mathbf{k}, \omega) = & \frac{1}{N^2} \sum_{\mathbf{p}, \mathbf{q}} \Lambda(\mathbf{q}, \mathbf{p}, \mathbf{k}) \frac{B_{\mathbf{q}+\mathbf{k}} Z_{aF}^2 \bar{\Delta}_{aZ}(\mathbf{p}) \bar{\Delta}_{aZ}(\mathbf{p} + \mathbf{q})}{\omega_{\mathbf{q}+\mathbf{k}} 4 E_{\mathbf{p}} E_{\mathbf{p}+\mathbf{q}}} \left[\frac{F_s^{(1)}(\mathbf{k}, \mathbf{p}, \mathbf{q})}{\omega^2 - (E_{\mathbf{p}} - E_{\mathbf{p}+\mathbf{q}} + \omega_{\mathbf{q}+\mathbf{k}})^2} + \frac{F_s^{(2)}(\mathbf{k}, \mathbf{p}, \mathbf{q})}{\omega^2 - (E_{\mathbf{p}+\mathbf{q}} - E_{\mathbf{p}} + \omega_{\mathbf{q}+\mathbf{k}})^2} \right. \\ & \left. + \frac{F_s^{(3)}(\mathbf{k}, \mathbf{p}, \mathbf{q})}{\omega^2 - (E_{\mathbf{p}} + E_{\mathbf{p}+\mathbf{q}} + \omega_{\mathbf{q}+\mathbf{k}})^2} + \frac{F_s^{(4)}(\mathbf{k}, \mathbf{p}, \mathbf{q})}{\omega^2 - (E_{\mathbf{p}+\mathbf{q}} + E_{\mathbf{p}} - \omega_{\mathbf{q}+\mathbf{k}})^2} \right], \quad (9) \end{aligned}$$

where $\Lambda(\mathbf{q}, \mathbf{p}, \mathbf{k}) = [(Zt\gamma_{\mathbf{k}-\mathbf{p}} - Zt'\gamma_{\mathbf{k}-\mathbf{p}}')^2 + (Zt\gamma_{\mathbf{q}+\mathbf{p}+\mathbf{k}} - Zt'\gamma_{\mathbf{q}+\mathbf{p}+\mathbf{k}}')^2]$, N is the number of sites, $F_s^{(1)}(\mathbf{k}, \mathbf{p}, \mathbf{q}) = (E_{\mathbf{p}} - E_{\mathbf{p}+\mathbf{q}} + \omega_{\mathbf{q}+\mathbf{k}}) \times \{n_B(\omega_{\mathbf{q}+\mathbf{k}})[n_F(E_{\mathbf{p}}) - n_F(E_{\mathbf{p}+\mathbf{q}})] - n_F(E_{\mathbf{p}+\mathbf{q}})n_F(-E_{\mathbf{p}})\}$, $F_s^{(2)}(\mathbf{k}, \mathbf{p}, \mathbf{q}) = (E_{\mathbf{p}+\mathbf{q}} - E_{\mathbf{p}} + \omega_{\mathbf{q}+\mathbf{k}})\{n_B(\omega_{\mathbf{q}+\mathbf{k}})[n_F(E_{\mathbf{p}+\mathbf{q}}) - n_F(E_{\mathbf{p}})] - n_F(E_{\mathbf{p}})n_F(-E_{\mathbf{p}+\mathbf{q}})\}$, $F_s^{(3)}(\mathbf{k}, \mathbf{p}, \mathbf{q}) = (E_{\mathbf{p}} + E_{\mathbf{p}+\mathbf{q}} + \omega_{\mathbf{q}+\mathbf{k}})\{n_B(\omega_{\mathbf{q}+\mathbf{k}})[n_F(-E_{\mathbf{p}}) - n_F(E_{\mathbf{p}+\mathbf{q}})] + n_F(-E_{\mathbf{p}+\mathbf{q}})n_F(-E_{\mathbf{p}})\}$, $F_s^{(4)}(\mathbf{k}, \mathbf{p}, \mathbf{q}) = (E_{\mathbf{p}} + E_{\mathbf{p}+\mathbf{q}} - \omega_{\mathbf{q}+\mathbf{k}}) \times \{n_B(\omega_{\mathbf{q}+\mathbf{k}})[n_F(-E_{\mathbf{p}}) - n_F(E_{\mathbf{p}+\mathbf{q}})] - n_F(E_{\mathbf{p}+\mathbf{q}})n_F(E_{\mathbf{p}})\}$, $\bar{\Delta}_{aZ}(\mathbf{k}) = Z_{aF}\bar{\Delta}_a(\mathbf{k})$ with $\bar{\Delta}_a(\mathbf{k}) = \bar{\Delta}_a[\gamma_{\mathbf{k}}^{(d)} - B\gamma_{\mathbf{k}}^{(2d)}]$, the dressed charge carrier quasiparticle spectrum $E_{\mathbf{k}} = \sqrt{\xi_{\mathbf{k}}^2 + |\bar{\Delta}_{aZ}(\mathbf{k})|^2}$, $\xi_{\mathbf{k}} = Z_{aF}\xi_{\mathbf{k}}$, and the MF dressed charge carrier excitation spectrum $\xi_{\mathbf{k}} = Zt\chi_1\gamma_{\mathbf{k}} - Zt'\chi_2\gamma_{\mathbf{k}}' - \mu$. The dressed charge carrier quasiparticle coherent weight Z_{aF} and effective dressed charge carrier gap parameters $\bar{\Delta}_a$ and B are determined by the following three equations:¹²

$$1 = \frac{1}{N^3} \sum_{\mathbf{k}, \mathbf{q}, \mathbf{p}} \Gamma_{\mathbf{k}+\mathbf{q}}^2 [\gamma_{\mathbf{k}}^{(d)} - B\gamma_{\mathbf{k}}^{(2d)}] \gamma_{\mathbf{k}-\mathbf{p}+\mathbf{q}}^{(d)} \frac{Z_{aF}^2 B_{\mathbf{q}} B_{\mathbf{p}}}{E_{\mathbf{k}} \omega_{\mathbf{q}} \omega_{\mathbf{p}}} \left[\frac{F_1^{(1)}(\mathbf{k}, \mathbf{q}, \mathbf{p})}{(\omega_{\mathbf{p}} - \omega_{\mathbf{q}})^2 - E_{\mathbf{k}}^2} - \frac{F_1^{(2)}(\mathbf{k}, \mathbf{q}, \mathbf{p})}{(\omega_{\mathbf{p}} + \omega_{\mathbf{q}})^2 - E_{\mathbf{k}}^2} \right], \quad (10)$$

$$B = -\frac{1}{N^3} \sum_{\mathbf{k}, \mathbf{q}, \mathbf{p}} \Gamma_{\mathbf{k}+\mathbf{q}}^2 [\gamma_{\mathbf{k}}^{(d)} - B\gamma_{\mathbf{k}}^{(2d)}] \gamma_{\mathbf{k}-\mathbf{p}+\mathbf{q}}^{(2d)} \frac{Z_{aF}^2 B_{\mathbf{q}} B_{\mathbf{p}}}{E_{\mathbf{k}} \omega_{\mathbf{q}} \omega_{\mathbf{p}}} \left[\frac{F_1^{(1)}(\mathbf{k}, \mathbf{q}, \mathbf{p})}{(\omega_{\mathbf{p}} - \omega_{\mathbf{q}})^2 - E_{\mathbf{k}}^2} - \frac{F_1^{(2)}(\mathbf{k}, \mathbf{q}, \mathbf{p})}{(\omega_{\mathbf{p}} + \omega_{\mathbf{q}})^2 - E_{\mathbf{k}}^2} \right], \quad (11)$$

$$\begin{aligned} \frac{1}{Z_{aF}} = 1 + \frac{1}{N^2} \sum_{\mathbf{q}, \mathbf{p}} \Gamma_{\mathbf{p}+\mathbf{k}_0}^2 Z_{aF} \frac{B_{\mathbf{q}} B_{\mathbf{p}}}{4\omega_{\mathbf{q}} \omega_{\mathbf{p}}} & \left[\frac{F_2^{(1)}(\mathbf{q}, \mathbf{p})}{(\omega_{\mathbf{p}} - \omega_{\mathbf{q}} - E_{\mathbf{p}-\mathbf{q}+\mathbf{k}_0})^2} + \frac{F_2^{(2)}(\mathbf{q}, \mathbf{p})}{(\omega_{\mathbf{p}} - \omega_{\mathbf{q}} + E_{\mathbf{p}-\mathbf{q}+\mathbf{k}_0})^2} \right. \\ & \left. + \frac{F_2^{(3)}(\mathbf{q}, \mathbf{p})}{(\omega_{\mathbf{p}} + \omega_{\mathbf{q}} - E_{\mathbf{p}-\mathbf{q}+\mathbf{k}_0})^2} + \frac{F_2^{(4)}(\mathbf{q}, \mathbf{p})}{(\omega_{\mathbf{p}} + \omega_{\mathbf{q}} + E_{\mathbf{p}-\mathbf{q}+\mathbf{k}_0})^2} \right], \quad (12) \end{aligned}$$

where $\Gamma_{\mathbf{k}+\mathbf{q}} = Zt\gamma_{\mathbf{k}+\mathbf{q}} - Zt'\gamma'_{\mathbf{k}+\mathbf{q}}$, $F_1^{(1)}(\mathbf{k}, \mathbf{q}, \mathbf{p}) = (\omega_{\mathbf{p}} - \omega_{\mathbf{q}}) \times [n_B(\omega_{\mathbf{q}}) - n_B(\omega_{\mathbf{p}})] [1 - 2n_F(E_{\mathbf{k}})] + E_{\mathbf{k}} [n_B(\omega_{\mathbf{p}}) n_B(-\omega_{\mathbf{q}}) + n_B(\omega_{\mathbf{q}}) n_B(-\omega_{\mathbf{p}})]$, $F_1^{(2)}(\mathbf{k}, \mathbf{q}, \mathbf{p}) = (\omega_{\mathbf{p}} + \omega_{\mathbf{q}}) [n_B(-\omega_{\mathbf{p}}) - n_B(\omega_{\mathbf{q}})] \times [1 - 2n_F(E_{\mathbf{k}})] + E_{\mathbf{k}} [n_B(\omega_{\mathbf{p}}) n_B(\omega_{\mathbf{q}}) + n_B(-\omega_{\mathbf{p}}) n_B(-\omega_{\mathbf{q}})]$, $F_2^{(1)}(\mathbf{q}, \mathbf{p}) = n_F(E_{\mathbf{p}-\mathbf{q}+\mathbf{k}_0}) [n_B(\omega_{\mathbf{q}}) - n_B(\omega_{\mathbf{p}})] - n_B(\omega_{\mathbf{p}}) n_B(-\omega_{\mathbf{q}})$, $F_2^{(2)}(\mathbf{q}, \mathbf{p}) = n_F(E_{\mathbf{p}-\mathbf{q}+\mathbf{k}_0}) [n_B(\omega_{\mathbf{p}}) - n_B(\omega_{\mathbf{q}})] - n_B(\omega_{\mathbf{q}}) n_B(-\omega_{\mathbf{p}})$, $F_2^{(3)}(\mathbf{q}, \mathbf{p}) = n_F(E_{\mathbf{p}-\mathbf{q}+\mathbf{k}_0}) [n_B(\omega_{\mathbf{q}}) - n_B(-\omega_{\mathbf{p}})] + n_B(\omega_{\mathbf{p}}) n_B(\omega_{\mathbf{q}})$, $F_2^{(4)}(\mathbf{q}, \mathbf{p}) = n_F(E_{\mathbf{p}-\mathbf{q}+\mathbf{k}_0}) [n_B(-\omega_{\mathbf{q}}) - n_B(\omega_{\mathbf{p}})] + n_B(-\omega_{\mathbf{p}}) n_B(-\omega_{\mathbf{q}})$, $\mathbf{k}_0 = [\pi, 0]$, and $n_B(\omega)$ and $n_F(\omega)$ are the boson and fermion distribution functions, respectively. These three equations must be solved self-consistently in combination with other equations as in the hole-doped case;¹² then, all order parameters, decoupling parameter α , and chemical potential μ are determined by the self-consistent calculation. In this sense, our above self-consistent calculation for the DSSF is controllable without using adjustable parameters, which has also been confirmed by a similar self-consistent calculation for the DSSF in the case of the hole-doped cuprate superconductors,¹² where a detailed description of this self-consistent method for the DSSF within the framework of the kinetic energy driven superconductivity has been given.

III. DOPING AND ENERGY DEPENDENT INCOMMENSURATE MAGNETIC SCATTERING AND COMMENSURATE RESONANCE

We are now ready to discuss the doping and energy dependence of the dynamical spin response in the electron-doped cuprate superconductors in the SC state. In Fig. 1, we plot the DSSF [Eq. (6)] of the electron-doped cuprate superconductors in the (k_x, k_y) plane in the electron doping $x = 0.15$ with temperature $T = 0.002J$ for parameters $t/J = -2.5$ and $t'/t = 0.3$ at energies (a) $\omega = 0.07J$, (b) $\omega = 0.12J$, and (c) $\omega = 0.36J$, where the self-consistently obtained values of the effective dressed charge carrier gap parameters $\bar{\Delta}_a$ and B from Eqs. (10) and (11) are $\bar{\Delta}_a = 0.1J$ and $B = 0.06J$. As seen from Fig. 1, the distinct feature of the present result is the presence of a commensurate-IC transition in the spin fluctuation geometry, where the magnetic excitations disperse with energy. To show this point clearly, we plot the evolution of

the magnetic scattering peaks with energy at $x = 0.15$ with $T = 0.002J$ for $t/J = -2.5$ and $t'/t = 0.3$ in Fig. 2. For comparison, the corresponding result of the evolution of the magnetic scattering peaks with energy at $x = 0.15$ with $T = 0.002J$ for $t/J = -2.5$ and $t'/t = 0.3$ with the monotonic d -wave SC gap function (dotted line) and the experimental result⁸ (inset) of the electron-doped $\text{Pr}_{0.88}\text{LaCe}_{0.12}\text{CuO}_{4-\delta}$ in the SC state are also shown in Fig. 2. For the case with the nonmonotonic d -wave gap function, the commensurate magnetic scattering consists of a strong peak at $[1/2, 1/2]$ (hereafter, we use the units of $[2\pi, 2\pi]$) at low energy ($\omega < 0.12J$). This broad commensurate magnetic scattering differs from the hole-doped side, where the IC magnetic scattering appears at low energy. With increase in energy for $\omega > 0.12J$, the IC magnetic scattering peaks appear. Although the main IC magnetic peaks are located at $[(1 \pm \delta)/2, 1/2]$ and $[1/2, (1 \pm \delta)/2]$ with δ as the IC parameter, these main IC magnetic peaks and other satellite IC magnetic peaks lie on a ring of δ and are symmetric around $[1/2, 1/2]$. This ring continues to disperse outward with increasing energy; then, the magnetic excitation spectrum has a dispersion similar to the spin wave, in qualitative agreement with the INS experimental data.⁸ However, for the case with the monotonic d -wave gap function, the IC magnetic scattering peaks appear at very low energies ($\omega < 0.07J$), and then the range of the low energy commensurate magnetic scattering is narrowed. These results for both nonmonotonic and monotonic d -wave gap functions show obviously that the higher harmonic term in the nonmonotonic d -wave gap function [Eq. (5)] mainly affects the low energy behavior of the dynamical spin response.

For determining the commensurate magnetic resonance energy in the SC state, we have made a series of calculations for the intensities of the DSSF in the SC state with the nonmonotonic d -wave gap function and normal state; the differences between the SC state and normal state intensities at different energies in the low energy commensurate scattering range and the results of the intensities of the DSSF in the (a) SC state, (b) normal state, and (c) the differences between the SC state and normal state intensities as a function of energy at $x = 0.15$ with $T = 0.002J$ for $t/J = -2.5$ and $t'/t = 0.3$ are plotted in Fig. 3. For comparison, the corresponding

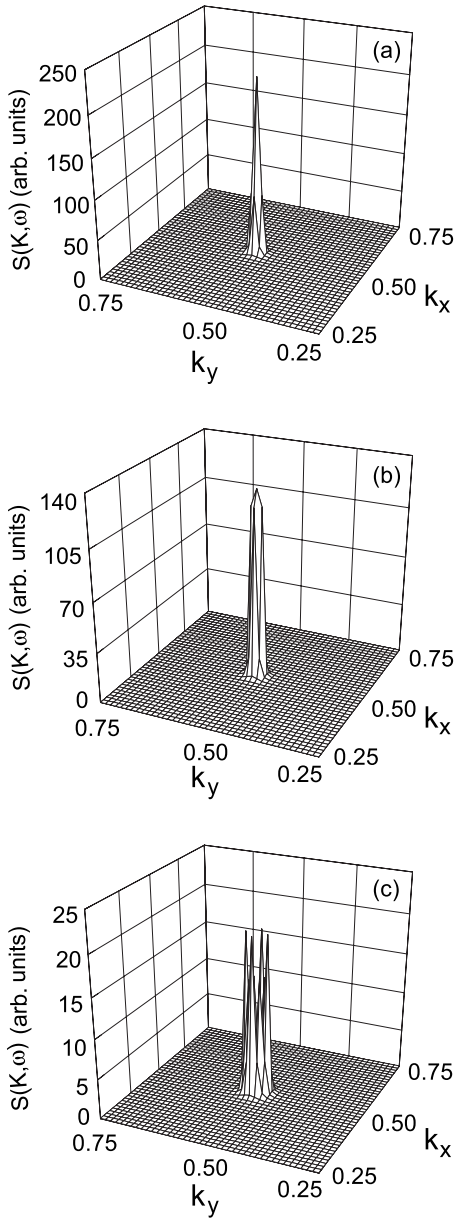


FIG. 1. The dynamical spin structure factor $S(\mathbf{k}, \omega)$ in the (k_x, k_y) plane at $x=0.15$ with $T=0.002J$ for $t/J=-2.5$ and $t'/t=0.3$ at (a) $\omega=0.07J$, (b) $\omega=0.12J$, and (c) $\omega=0.36J$.

experimental data¹⁰ of the differences between the SC state and normal state intensities for $\text{Pr}_{0.88}\text{LaCe}_{0.12}\text{CuO}_{4-\delta}$ are also shown in Fig. 3(c) (inset). Obviously, the corresponding intensity of the DSSF in the normal state is much smaller than that in the SC state; then, the commensurate resonance is essentially determined by the intensities of the DSSF in the SC state. In this case, a commensurate resonance peak centered at $\omega_r=0.07J$ is obtained from Fig. 3(c). In particular, this magnetic resonance energy is located among the low energy commensurate scattering range. Using a reasonable estimative value of $J \sim 150$ meV in the electron-doped cuprate superconductors,⁸ the present result of the resonance energy $\omega_r=0.07J \approx 10.5$ meV is in quantitative agreement with the resonance energy ≈ 11 meV observed¹⁰ in $\text{Pr}_{0.88}\text{LaCe}_{0.12}\text{CuO}_{4-\delta}$. Furthermore, we also find that the

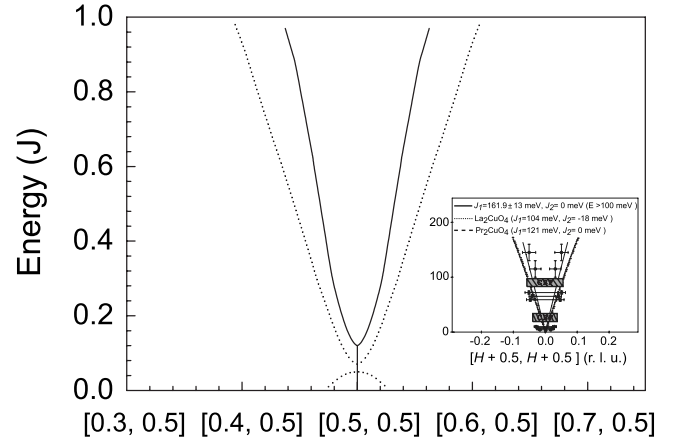


FIG. 2. The energy dependence of the position of the scattering peaks at $x=0.15$ with $T=0.002J$ for $t/J=-2.5$ and $t'/t=0.3$. The dotted lines correspond to the monotonic d -wave SC gap function. Inset: The corresponding experimental result of $\text{Pr}_{0.88}\text{LaCe}_{0.12}\text{CuO}_{4-\delta}$ taken from Ref. 8.

value of the resonance energy ω_r is dependent on the next-neighbor hopping t' , i.e., with increasing t' , the value of the resonance energy ω_r increases. Since the value of t' is believed to vary somewhat from compound to compound, therefore, there are different values of the resonance energy ω_r for different families of the electron-doped cuprate superconductors. However, there is a substantial difference between theory and experiment; namely, the differences between SC state and normal state intensities in the DSSF show a flat behavior for $\text{Pr}_{0.88}\text{LaCe}_{0.12}\text{CuO}_{4-\delta}$ at low energies below 5 meV,¹⁰ while the calculation anticipates that the differences of the SC state and normal state intensities linearly increase from the zero energy toward the resonance peak. However, upon a closer examination, one sees immediately that the main difference is due to the fact that the difference of the SC state and normal state intensities linearly increases at too low energies in the theoretical consideration. The actual range of rapid growth of the differences of the SC state and normal state intensities with energy (around 5–16 meV) is very similar in theory and experiments. We emphasize that although the simple t - t' - J model [Eq. (1)] cannot be regarded as a comprehensive model for a quantitative comparison with the electron-doped cuprate superconductor $\text{Pr}_{0.88}\text{LaCe}_{0.12}\text{CuO}_{4-\delta}$, our present results for the SC state are in qualitative agreement with the major experimental observations on the electron-doped cuprate superconductor $\text{Pr}_{0.88}\text{LaCe}_{0.12}\text{CuO}_{4-\delta}$.⁸⁻¹⁰ Very recently, this magnetic resonance in $\text{Pr}_{0.88}\text{LaCe}_{0.12}\text{CuO}_{4-\delta}$ in the SC state has also been studied by considering the dynamical spin susceptibility within the random phase approximation,²³ where similar nonmonotonic d -wave gap function [Eq. (5)] has been used in the calculation. They²³ argued that the observed magnetic resonance peak in $\text{Pr}_{0.88}\text{LaCe}_{0.12}\text{CuO}_{4-\delta}$ is due to an overdamped spin excitation located near the particle-hole continuum, and the calculated results are consistent with ours.

Now, we turn to discuss the doping dependence of the commensurate magnetic resonance energy. We have also made a series of calculations for the resonance energy at

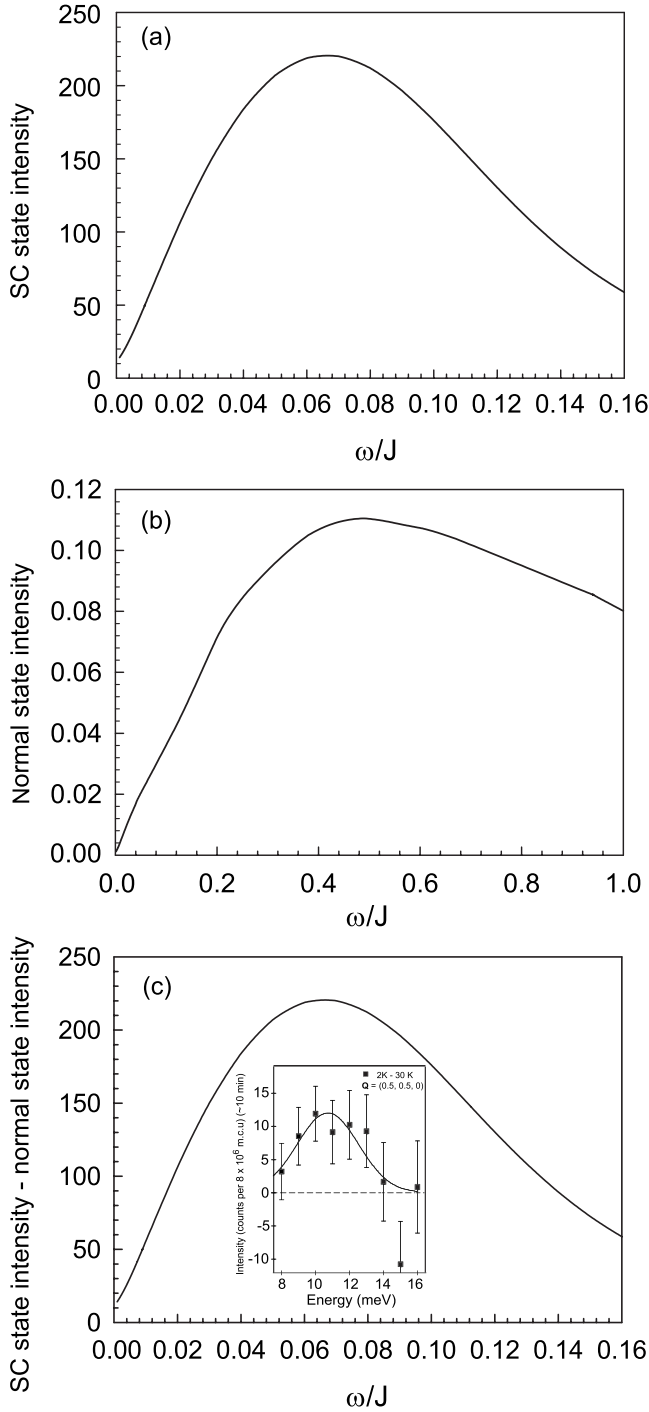


FIG. 3. The intensities of the dynamical spin structure factor in the (a) SC state and (b) normal state and (c) the differences between the SC state and normal state intensities as a function of energy at $x=0.15$ with $T=0.002J$ for $t/J=-2.5$ and $t'/t=0.3$. Inset: The corresponding experimental result of $\text{Pr}_{0.88}\text{LaCe}_{0.12}\text{CuO}_{4-\delta}$ taken from Ref. 10.

different doping, and the result of the resonance energy ω_r at $T=0.002J$ and SC transition temperature T_c as a function of the electron doping x for $t/J=-2.5$ and $t'/t=0.3$ is plotted in Fig. 4. For comparison, the corresponding experimental result of the SC transition temperature of $\text{Pr}_{2-x}\text{Ce}_x\text{CuO}_{4-\delta}$ (Ref.

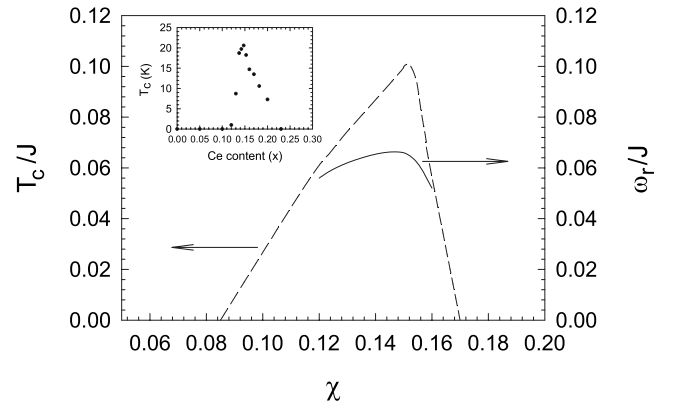


FIG. 4. The resonance energy ω_r (solid line) at $T=0.002J$ and superconducting transition temperature T_c (dashed line) as a function of x for $t/J=-2.5$ and $t'/t=0.3$. Inset: The corresponding experimental result of the superconducting transition temperature of $\text{Pr}_{2-x}\text{Ce}_x\text{CuO}_{4-\delta}$ taken from Ref. 24.

24) is also shown in the same figure (inset). Our results show that in analogy to the doping dependent SC transition temperature,²⁴ the magnetic resonance energy ω_r increases with increasing doping in the underdoped regime, then reaches a maximum in the optimal doping, then decreases in the overdoped regime. In comparison with the previous results for the hole-doped case,¹² our present results also show that the commensurate magnetic resonance is a common feature for cuprate superconductors irrespective of the hole doping or electron doping, while the commensurate magnetic scattering at low energy in the present electron-doped case indicates that the intimate connection between the IC magnetic scattering and resonance in the hole-doped side at low energy is not a universal feature. In other words, the resonance energy itself is intimately related to superconductivity; other details such as the incommensurability and hour-glass dispersion found in different cuprate superconductors may not be fundamental to superconductivity.⁸⁻¹⁰

The essential physics of the doping and energy dependence of the dynamical spin response in the electron-doped cuprate superconductor $\text{Pr}_{0.88}\text{LaCe}_{0.12}\text{CuO}_{4-\delta}$ in the SC state is the same as in the hole-doped case,¹² except the nonmonotonic d -wave gap function form [Eq. (5)]. Although the momentum dependence of the SC gap function [Eq. (5)] is basically consistent with the d -wave symmetry, it obviously deviates from the monotonic d -wave SC gap function.²¹ This is different from the hole-doped case, where the momentum dependence of the monotonic d -wave SC gap function is observed.²⁰ As seen from Fig. 2, the higher harmonic term in Eq. (5) mainly affects the low energy behavior of the dynamical spin response, i.e., the nonmonotonic d -wave SC gap function [Eq. (5)] in the electron-doped cuprate superconductors modulates the renormalized spin excitation spectrum in the electron-doped cuprate superconductors and therefore leads to the difference of the low energy dynamical spin response between the hole-doped and electron-doped cuprate superconductors in the SC state.

IV. SUMMARY AND DISCUSSIONS

In summary, we have shown very clearly in this paper that if the nonmonotonic d -wave SC gap function is taken into

account in the framework of the kinetic energy driven SC mechanism, the DSSF of the t - t' - J model calculated in terms of the collective mode in the dressed charge carrier particle-particle channel *per se* can correctly reproduce all main features found in the INS measurements on the electron-doped cuprate superconductor $\text{Pr}_{0.88}\text{LaCe}_{0.12}\text{CuO}_{4-\delta}$ including the energy dependence of the commensurate magnetic scattering and resonance at low energy and IC magnetic scattering at high energy, without using adjustable parameters. We believe that the commensurate magnetic resonance is a universal feature of cuprate superconductors, as shown by the INS experiments on the hole-doped cuprate superconductors $\text{YBa}_2\text{Cu}_3\text{O}_{7-\delta}$ ⁴, $\text{La}_{2-x}\text{Sr}_x\text{CuO}_4$ ⁵, $\text{Tl}_2\text{Ba}_2\text{CuO}_{6+\delta}$ ⁶ and $\text{Bi}_2\text{Sr}_2\text{CaCu}_2\text{O}_{8+\delta}$ (Ref. 6) and electron-doped cuprate superconductors $\text{Pr}_{1-x}\text{LaCe}_x\text{CuO}_{4-\delta}$ (Refs. 8–10) and $\text{Nd}_{2-x}\text{Ce}_x\text{CuO}_{4-\delta}$ ²⁵. The theory also predicts a dome shaped doping dependent magnetic resonance energy, which should be verified by further experiments.

Within the framework of the kinetic energy driven SC mechanism, we²⁶ have studied the electronic structure of the electron-doped cuprate superconductors in the SC state. It is shown that although there is an electron-hole asymmetry in the phase diagram, the electronic structure of the electron-doped cuprates in the SC state is similar to that in the hole-doped case. In particular, it is also shown that the higher harmonic term in Eq. (5) mainly affects the low energy spec-

tral weight, i.e., the low energy spectral weight increases when the higher harmonic term is considered, while the position of the SC quasiparticle peak is slightly shifted away from the Fermi energy.²⁶ This is consistent with the present result of the spin dynamics, and both studies indicate that the higher harmonic term in Eq. (5) mainly affects the low energy behavior of the systems.

Finally, we have noted that the differences of the intensities between SC and normal states become negative for the electron-doped cuprate superconductor $\text{Nd}_{1.85}\text{Ce}_{0.15}\text{CuO}_{4-\delta}$ at low energies below 5 meV,²⁵ which shows that the DSSF intensity at energies below 5 meV is suppressed in the SC state. Although it has been argued that this unusual behavior of the dynamical spin response of $\text{Nd}_{1.85}\text{Ce}_{0.15}\text{CuO}_{4-\delta}$ may be related to the spin gap,^{23,25} the physical reason for this unusual behavior is still not clear. These and the related issues are under investigation now.

ACKNOWLEDGMENTS

The authors would like to thank P. Dai for the helpful discussions. This work was supported by the National Natural Science Foundation of China under Grant Nos. 90403005 and 10774015 and the funds from the Ministry of Science and Technology of China under Grant Nos. 2006CB601002 and 2006CB921300.

*Author to whom correspondence should be addressed.

¹J. G. Bednorz and K. A. Müller, *Z. Phys. B: Condens. Matter* **64**, 189 (1986); Y. Tokura, H. Takagi, and S. Uchida, *Nature (London)* **337**, 345 (1989).

²See, e.g., M. A. Kastner, R. J. Birgeneau, G. Shirane, and Y. Endoh, *Rev. Mod. Phys.* **70**, 897 (1998), and references therein.

³See, e.g., A. Damascelli, Z. Hussain, and Z. X. Shen, *Rev. Mod. Phys.* **75**, 473 (2003), and references therein.

⁴P. Dai, H. A. Mook, R. D. Hunt, and F. Doğan, *Phys. Rev. B* **63**, 054525 (2001); M. Arai, T. Nishijima, Y. Endoh, T. Egami, S. Tajima, K. Tomimoto, Y. Shiohara, M. Takahashi, A. Garrett, and S. M. Bennington, *Phys. Rev. Lett.* **83**, 608 (1999).

⁵K. Yamada, C. H. Lee, K. Kurahashi, J. Wada, S. Wakimoto, S. Ueki, H. Kimura, Y. Endoh, S. Hosoya, G. Shirane, R. J. Birgeneau, M. Greven, M. A. Kastner, and Y. J. Kim, *Phys. Rev. B* **57**, 6165 (1998); S. Wakimoto, H. Zhang, K. Yamada, I. Swainson, H. Kim, and R. J. Birgeneau, *Phys. Rev. Lett.* **92**, 217004 (2004); N. B. Christensen, D. F. McMorrow, H. M. Rønnow, B. Lake, S. M. Hayden, G. Aeppli, T. G. Perring, M. Mangkorn-tong, M. Nohara, and H. Tagaki, *ibid.* **93**, 147002 (2004).

⁶P. Bourges, B. Keimer, S. Pailhès, L. P. Regnault, Y. Sidis, and C. Ulrich, *Physica C* **424**, 45 (2005); P. Bourges, Y. Sidis, H. F. Fong, L. P. Regnault, J. Bossy, A. Ivanov, and B. Keimer, *Science* **288**, 1234 (2000); H. He, Y. Sidis, P. Bourges, G. D. Gu, A. Ivanov, N. Koshizuka, B. Liang, C. T. Lin, L. P. Regnault, E. Schoenher, and B. Keimer, *Phys. Rev. Lett.* **86**, 1610 (2001).

⁷S. M. Hayden, H. A. Mook, P. Dai, T. G. Perring, and F. Dogan, *Science* **429**, 531 (2004); V. Hinkov, S. Pailhès, P. Bourges, Y. Sidis, A. Ivanov, A. Kulakov, C. T. Lin, D. P. Chen, C. Bern-

hard, and B. Keimer, *Nature (London)* **430**, 650 (2004); C. Stock, W. J. L. Buyers, R. A. Cowley, P. S. Clegg, R. Coldea, C. D. Frost, R. Liang, D. Peets, D. Bonn, W. N. Hardy, and R. J. Birgeneau, *Phys. Rev. B* **71**, 024522 (2005).

⁸Stephen D. Wilson, Shiliang Li, Hyungje Woo, Pengcheng Dai, H. A. Mook, C. D. Frost, Seiki Komiya, and Yoichi Ando, *Phys. Rev. Lett.* **96**, 157001 (2006).

⁹Stephen D. Wilson, Shiliang Li, Pengcheng Dai, Wei Bao, Jae-Ho Chung, H. J. Kang, Seung-Hun Lee, Seiki Komiya, Yoichi Ando, and Qimiao Si, *Phys. Rev. B* **74**, 144514 (2006).

¹⁰Stephen D. Wilson, Pengcheng Dai, Shiliang Li, Songxue Chi, H. J. Kang, and J. W. Lynn, *Nature (London)* **442**, 59 (2006).

¹¹Shiping Feng, *Phys. Rev. B* **68**, 184501 (2003).

¹²Shiping Feng, Tianxing Ma, and Huaiming Guo, *Physica C* **436**, 14 (2006); Shiping Feng, Tianxing Ma, and Xintian Wu, *Phys. Lett. A* **352**, 438 (2006); Shiping Feng and Tianxing Ma, in *Superconductivity Research Horizons*, edited by Eugene H. Peterson (Nova Science, New York, 2007), Chap. 5, p. 129.

¹³C. Kim, P. J. White, Z. X. Shen, T. Tohyama, Y. Shibata, S. Maekawa, B. O. Wells, Y. J. Kim, R. J. Birgeneau, and M. A. Kastner, *Phys. Rev. Lett.* **80**, 4245 (1998).

¹⁴M. S. Hybertsen, E. B. Stechel, M. Schluter, and D. R. Jennison, *Phys. Rev. B* **41**, 11068 (1990).

¹⁵E. Pavarini, I. Dasgupta, T. Saha-Dasgupta, O. Jepsen, and O. K. Andersen, *Phys. Rev. Lett.* **87**, 047003 (2001).

¹⁶R. J. Gooding, K. J. E. Vos, and P. W. Leung, *Phys. Rev. B* **50**, 12866 (1994).

¹⁷C. Kusko, R. S. Markiewicz, M. Lindroos, and A. Bansil, *Phys. Rev. B* **66**, 140513(R) (2002); Huaiming Guo and Shiping Feng,

- Phys. Lett. A **355**, 473 (2006).
- ¹⁸Shiping Feng, Jihong Qin, and Tianxing Ma, *J. Phys.: Condens. Matter* **16**, 343 (2004); Shiping Feng, Tianxing Ma, and Jihong Qin, *Mod. Phys. Lett. B* **17**, 361 (2003).
- ¹⁹See, e.g., Shiping Feng, Huaiming Guo, Yu Lan, and Li Cheng, arXiv:0710.5258 *Int. J. Mod. Phys. B* (to be published).
- ²⁰H. Ding, M. R. Norman, J. C. Campuzano, M. Randeria, A. F. Bellman, T. Yokoya, T. Takahashi, T. Mochiku, and K. Kawakami, *Phys. Rev. B* **54**, R9678 (1996).
- ²¹H. Matsui, K. Terashima, T. Sato, T. Takahashi, M. Fujita, and K. Yamada, *Phys. Rev. Lett.* **95**, 017003 (2005).
- ²²Tianxing Ma and Shiping Feng, *Phys. Lett. A* **339**, 131 (2007).
- ²³J.-P. Ismer, Ilya Eremin, Enrico Rossi, and Dirk K. Morr, *Phys. Rev. Lett.* **99**, 047005 (2007).
- ²⁴J. L. Peng, E. Maiser, T. Venkatesan, R. L. Greene, and G. Czjzek, *Phys. Rev. B* **55**, R6145 (1997).
- ²⁵Jun Zhao, Pengcheng Dai, Shiliang Li, Paul G. Freeman, Y. Onose, and Y. Tokura, *Phys. Rev. Lett.* **99**, 017001 (2007).
- ²⁶Li Cheng, Huaiming Guo, and Shiping Feng, *Phys. Lett. A* **366**, 137 (2007); Li Cheng and Shiping Feng (unpublished).